MINERALOGICAL MAGAZINE

VOLUME 53 NUMBER 372 SEPTEMBER 1989

Carbonatite-related contact metasomatism in the Fen complex, Norway: effects and petrogenetic implications

TOM ANDERSEN

Mineralogisk-Geologisk Museum, Sars gate 1, N-0562 Oslo 5, Norway

Abstract

In the Fen complex (Telemark, S.E. Norway), carbonatites of different compositions have penetrated feldspathic fenites (alkali feldspar(s) + aegirine augite ± alkali amphibole) or older carbonatites, inducing different types of contact metasomatic alterations in their wall-rocks. (1) *Pyroxene søvite* has induced alkali metasomatism (i.e. fenitization *s.s.*), with alkali feldspars remaining stable and aegirine-augite transformed to nearly pure aegirine. (2) *Søvite* and *dolomite carbonatite* with phlogopite and/or alkali or alkali-calcic amphibole have caused replacement of feldspathic fenite by phlogopite, i.e. magnesium metasomatism. (3) *Granular (dyke facies) ferrocarbonatite* has increased the ferromagnesian components in calcite in wall-rock søvite. (4) *Heterogeneous (pyroclastic) ferrocarbonatite* induced pseudomorphic replacement of phlogopite by chlorite (leaching of alkalis). The different contact metasomatic processes reflect contrasts in compositional character among carbonatite magmas in the Fen complex, which may be evaluated in terms of differences in alkali and magnesium carbonate activities. The different types of carbonatite magma represent the products of local evolutionary trends, and are genetically related to spatially associated silicate rocks, rather than to a single 'primitive' carbonatite parent magma.

KEYWORDS: carbonatite, metasomatism, fenite, Fen complex, Norway.

Introduction

ALL metasomatic processes related to the emplacement and crystallization of magma can convey important information about the geochemical character of the liquids responsible, especially when the alteration processes at the immediate contact between intrusions and country rocks (*contact metasomatism*) are taken into consideration. Such information is of great value for the discussion of the compositional evolution of carbonatite magmas, as carbonatites in many cases only preserve an incomplete memory of magmatic processes, due to late- or post-magmatic re-equilibration and loss of material (Gittins, 1979; Andersen, 1984; 1987*b*; Dawson *et al.*, 1987).

Carbonatite magmas are the results of complex chains of processes, involving liquid immiscibility between carbonate and silicate melts, fractional crystallization and exchange of components between magmas and fluid phases (e.g. Le Bas, 1977; Treiman and Essene, 1985). According to some authors, strongly alkaline carbonatite magmas with $Na_2CO_3 > CaCO_3$ (akin to the Oldoynio Lengai-type natrocarbonatite; Dawson, 1962) are parental to more common, alkali-poor carbonatites (e.g. *søvite*, i.e. calcite carbonatite). Alkali-rich carbonatite magmas are thought to evolve into normal, alkali-poor calcitic carbonatite magmas by loss of alkalis to magmatic fluids after initial formation of the carbonatite magma (Dawson, 1964; Gittins and McKie, 1980; Dawson *et al.*, 1987; Woolley, 1982; Le Bas, 1981, 1987). When brought into contact with less peralkaline wall-rocks, a fluid phase exsolving from a natrocarbonatite-type magma would deposit some of its alkali-content in minerals formed in metasomatic reactions. Hence, the presence of country rocks metasomatically enriched in alkalis next to carbonatite intrusions, is good evidence of high initial alkali concentrations in the carbonatite magmas.

Although alkali-enriched metasomatic rocks are widespread in carbonatite and alkaline silicate rock complexes, they are by no means the only metasomatic rocks formed in such settings (e.g. Andersen, 1984, 1986). The processes by which the alkali-poorer metasomatic rock-types form have not been investigated in any detail. The aim

Mineralogical Magazine, September 1989, Vol. 53, pp. 395–414

of the present study is therefore to characterize the metasomatic processes associated with different types of carbonatite intrusions, from field, petrographical and mineralogical data, and to explore the potential of these processes as indicators of magma composition and evolution. The Fen complex in Telemark, Norway is well suited for a case study of these processes, as it exhibits a varied suite of carbonatites and contact metasomatic rocks.

The Fen complex

The Fen complex (Fig. 1) was emplaced in the Cambrian (540–550 Ma, Andersen and Taylor, 1988; Andersen and Sundvoll, 1987; Dahlgren, 1987). It consists of a central carbonatite and alkaline silicate intrusive complex surrounded by metasomatized country rocks, and numerous minor satellite intrusions. The pioneering work of Brøgger (1921) established it among the type examples of its kind. Since that time, the geology, petrology and geochemistry of the complex have been extensively restudied (e.g. Sæther, 1957; Bergstøl and Svinndal, 1960; Barth and Ramberg, 1966; Kresten and Morogan, 1986; Andersen, 1983, 1984, 1986, 1987*a*,*b*, 1988; Andersen and Qvale, 1986).

The silicate members of the complex include ijolitic rocks (nepheline + sodic pyroxene), nepheline syenite and damtjernite, which is a phlogopite-bearing ultramafic lamprophyre (Dahlgren, 1987). Based on published petrographic observations and geochemical data, it is possible to divide the carbonatites into four 'groups', as indicated in Table 1. The group 1 carbonatites are spatially associated with ijolitic rocks and nepheline syenite, whereas the group 4 pyroclastic intrusions are associated with diatremes of damtjernite-like silicate rocks; each of these rock associations probably reflects close genetical relationships between the silicate and carbonatite members (Sæther, 1957; Mitchell and Brunfelt, 1975; Andersen and Qvale, 1986; Andersen, 1988).

The present level of erosion through the complex represents a section through the shallow crust (*ca.* 1–3 km, Sæther, 1957). Carbonatites are the most abundant magmatic rocks exposed within the central complex, constituting 60% of the total outcrop area, with intrusive silicate rocks amounting to less than 20%, and different types of metasomatically altered country rocks making up the rest. Gravimetric data indicate that the central complex is underlain by a cylindrical body of dense material, probably mafic silicate rocks, extending from a few hundred metres below the present surface to at least 15 km depth (Ramberg, 1973).

Metasomatic alteration

In the Fen complex, alkali-enriched metasomatic rocks are restricted to the western perimeter (Fig. 1). Such rocks associated with alkaline igneous rocks and/or carbonatites are known as *fenites*, and the process of their formation is referred to as *fenitization* (e.g. McKie, 1966; Verwoerd, 1966). These terms were introduced by Brøgger (1921) and were originally coined for alkali syenitic metasomatic rocks formed from a meta-granitic protolith by introduction of Na_2O and leaching of SiO_2. This definition has been considerably extended in later studies, to include (*a*) all alkali-metasomatized rocks, disregarding their actual composition or protolith (Verwoerd, 1966), or (*b*) all rocks metasomatized by emanations from alkaline silicate rocks or carbonatites, whether or not alkalis have been mobile (v. Eckermann, 1948; McKie, 1966; Heinrich, 1966). In the present paper, definition *a* is used, in agreement with Brøgger's (1921) conception of fenitization as a process involving alkali-enrichment.

Kresten (1988) distinguished between aureole fenites, produced by metasomatism extending tens to hundreds of metres from its magmatic source, and contact fenites, formed by processes at the wall-rock to intrusion interface only. The most important features of aureole (A) and contact (C) metasomatic processes in the Fen complex are summarized in Table 2. Contact fenitization induced by group 1 carbonatite intrusions will be discussed more fully along with other types of contact metasomatism below.

Sæther (1957), Kresten and Morogan (1986), Kresten (1988) and Morogan (1988) have presented field evidence, petrographical observations and geochemical data to support the hypothesis originally set out by Brøgger (1921), that most of the aureole fenites in the complex were formed by fluids originating from ijolitic and related alkaline silicate magmas, before the emplacement of the carbonatites, pyroxene søvite/silicosøvite magmas having only minor and local fenitizing influence. Verschure and Maijer (1984 and pers. comm.) have distinguished between two metasomatic events in the fenite aureole, the first (here called A_1) producing acmite or sodic amphibole, the second (A_2) forming stilpnomelane at the expense of these minerals. From their preliminary data (Verschure and Maijer, 1984), it is not clear whether the A_2 metasomatic episode involved introduction of alkalis, that is if it can be said to be a fenitization process in the restrictive terminology adopted here.

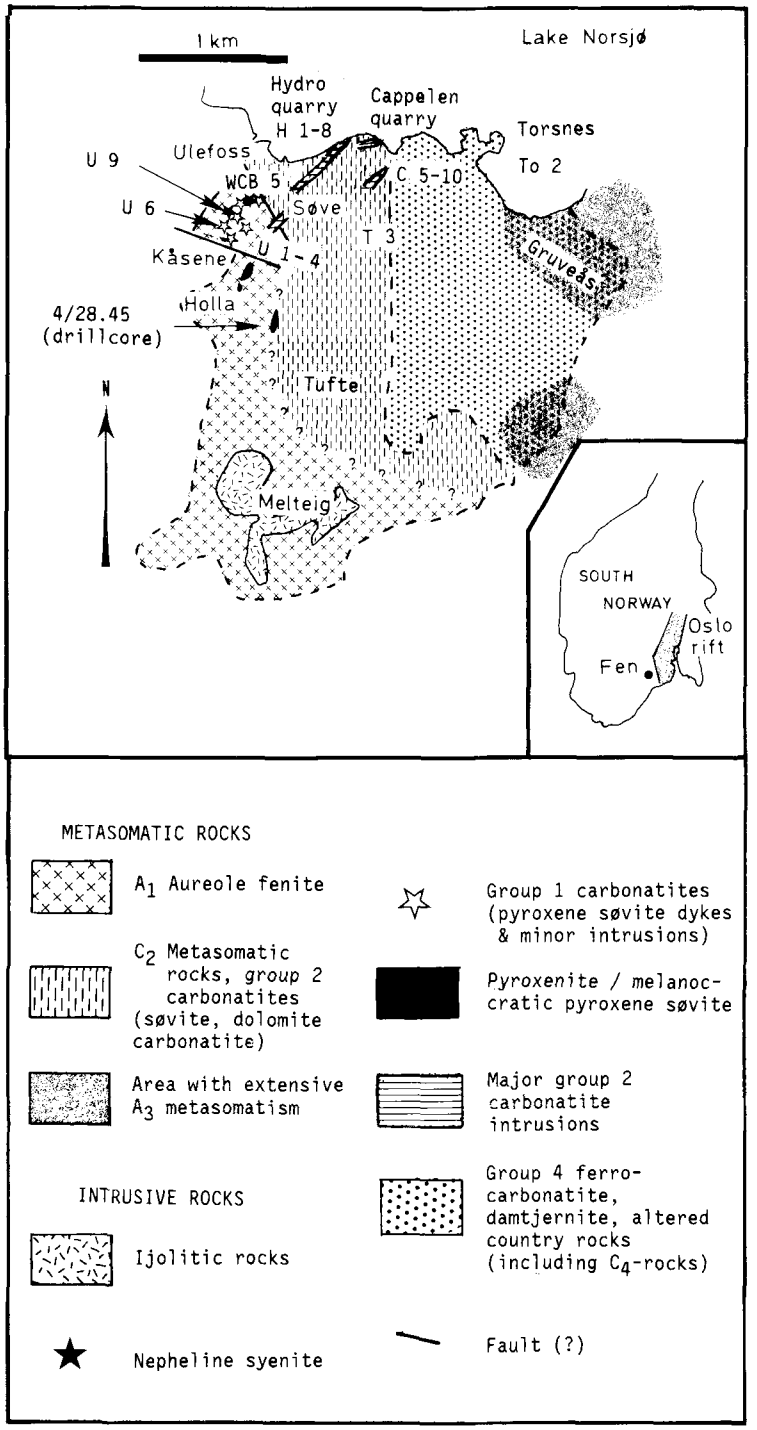

FIG. 1. Simplified geological map of the Fen complex, based on published maps by Sæther (1957), Dahlgren (1978) and Andersen and Qvale (1986). Sampling localities are indicated.

Table 1. Petrographic and geochemical characteristics of carbonatites in the Fen complex.

Group	Rock type	Characteristic minerals	Geochemistry
1	Søvite (Dykes)	Cc, sodian Cpx, Amph	
	Silicosøvite (Dykes)	± feldspar ± nepheline	$\varepsilon_{Sr} \leq -12$ at 540 Ma
			$\delta^{18}O_{SMOW}$ = +5.7
2	Søvite (Dykes)	Cc, Phl, Amph, Apt ± Dol	+ 5.7 - + 8 ‰
	Dolomite carbonatite (Dykes)	Dol, Phl, Apt, Cc	$\delta^{13}C_{PDB}$ =
			-3 to -5 ‰
	Apatite rock (Inclusions in carbonatite)	Apt, Mt, Phl, Amph, Cc, dol	1000-7000 ppm Sr 50-900 ppm Nd
3	Ferrocarbonatite (Dykes)	Ankerite, Mt, Py, Amph	
4	Ferrocarbonatite	Ankerite, Mt, Py, Chl	$\varepsilon_{Sr} > -10$ at 540 Ma
	(Pyroclastic intrusions)		$\delta^{18}O_{SMOW} > +8$ ‰
			$\delta^{13}C_{PDB} > -3$ ‰
			500-1700 ppm Sr 800-5000 ppm Nd

Petrographical data from Andersen (1984, 1986, 1988) and Andersen and Qvale (1986), geochemical data from Andersen (1987a). Abbreviations: Cpx = clinopyroxene, Amph = amphibole, Phl = phlogopite, Chl = chlorite, Apt = apatite, Cc = calcite, Dol = dolomite, Mt = magnetite, Py = pyrite. Underlined: characteristic / essential silicate mineral.

Table 2. Characteristics of metasomatic events in the Fen complex.

Event	Source	Affects	Characteristic minerals Before	After
Aureole metasomatism:				
A_1	Ijolite etc.	Granitic gneiss	Albite + microcline + quartz + biotite	Aegirine-augite, sodian amphibole, perthite
A_2	?	Al fenite	See above	Stilpnomelane
A_3	Groundwater	Ferrocarb.	Ankerite, magnetite, pyrite	Hematite + calcite + dolomite
		Granitic gneiss	Albite + microcline + quartz + biotite + hornblende	Quartz + calcite + albite + chlorite + hematite
Contact metasomatism:				
C_1	Group 1 carbonatite	A_1 fenite	See above	Acmite, alkali feldspar
C_2	Group 2 carbonatite	A_1 fenite	See above	Phlogopite + sodian amphibole + calcite
C_3	Group 3 carbonatite	Bi-amph søvite	Low Mg-Fe-Mn calcite	High Mg-Fe-Mn calcite
C_4	Group 4 carbonatite	Dol. carb.	Dolomite + phlogopite	Chlorite + calcite + dolomite + quartz

A third, later metasomatic event of aureole extent (A_3), was caused by interaction between rocks and groundwater-derived hydrothermal fluids infiltrating the eastern part of the complex, leading to oxidation of ferrocarbonatite to hematite carbonatite, locally known as 'rødberg', i.e. 'red-rock' (Sæther, 1957; Andersen, 1984, 1987*b*). The effect of the A_3 metasomatism can be traced for several hundred metres into the country rock gneiss (Andersen, 1984), and post-dates all but the latest pulses of pyroclastic group 4 ferrocarbonatite in the eastern part of the complex (Andersen and Qvale, 1986).

Contact metasomatism: geology and petrography

C_1: *contact metasomatism associated with group 1 carbonatites.* Dykes and veins of pyroxene søvite have intruded into A_1 fenites which consist of alkali feldspar + aegirine augite + sodic amphibole (Kresten and Morogan, 1986). The metasomatic effect of this type of carbonatite magma on the A_1 fenite is well illustrated by the contact relations of minor group 1 dykes and veins exposed in roadcuts at Ulefoss (Figs 1 and 2).

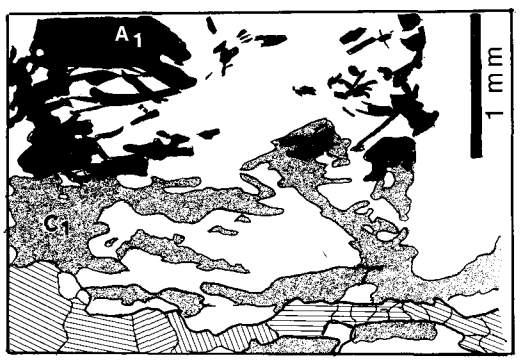

FIG. 2. The effect of C_1 contact metasomatism on clinopyroxene in A_1 aureole fenite, sample U6, drawn from photomicrograph. Phase identification: *Ruled*, calcite (in vein); *black*, dark green, pleochroic pyroxene; *shaded*, colourless, non-pleochroic pyroxene; *white*, alkali feldspar. The figure shows a clinopyroxene + feldspar vein belonging to the A_1 fenite (vein fenite; Kresten, 1988), cut by a pyroxene søvite vein (group 1). The A_1 pyroxene is characterized by Ac-contents well below 90 mole %. Approaching the carbonatite vein, the pyroxene crystals lose their colour, and change in composition to Ac > 90 mole %. The pyroxene habit is not affected by this process.

The pyroxene of the A_1 aureole fenite away from the pyroxene søvite is a green, pleochroic aegirine-augite (Fig. 2). At the interface to the carbonatite, and a few millimetres into the wall-rock, the pyroxene has been bleached, to become pale and non-pleochroic. In this process, pre-carbonatite pyroxene grain-shape and delicate structures such as 'comb-layering' along pre-C_1 veins in the fenite are retained undisturbed. The matrix feldspar of the A_1 fenite is a cloudy mesoperthite ($Ab_{>90}$ + $Or_{>90}$). At the contact with the carbonatite, this feldspar is overgrown by clear alkali feldspar. Microprobe analyses indicate a composition of $Ab_{25}Or_{75}$.

C_2: *contact metasomatism associated with group 2 carbonatites.* The wall-rock alterations caused by biotite søvite and dolomite carbonatite is of much greater intensity and areal extent than the small-scale contact metasomatism accompanying the pyroxene søvite. Relics of the A_1 fenite mineral assemblage (alkali feldspar + sodic pyroxene + sodic amphibole) can be found within the zones modified by C_2 contact metasomatism. Along the contacts of the carbonatites, the feldspathic A_1 fenite has been altered to dark aggregates of mica + amphibole + calcite + apatite (Fig. 3). At the contact with dykes or veins, the alteration reaches only millimetres to centimetres into the wallrock, as illustrated in Fig. 3. Near major intrusions or dyke-swarms (e.g. in the Cappelen quarry and S.E. of Ulefoss, the fenite is very thoroughly altered for metres away from the intrusive rocks, leaving only mantled relics of the A_1 aureole fenite.

C_3: *contact metasomatism associated with group 3 carbonatite.* In the Cappelen quarry, swarms of 1–10 mm wide, monomineralic ferrocarbonatite veins cut through søvite and altered fenite. The veins are continuous for several metres along strike, and not visibly connected to any larger ferrocarbonatite intrusions. The contact relations between the ferrocarbonatite veins and the søvite host-rock are illustrated in Fig. 4. All veins, even the thinnest, are surrounded by metasomatic zones, wider than the veins themselves, in which white, coarse-grained calcite of the søvite has recrystallized to grey, fine-grained calcite. The effects of C_3 contact metasomatism also show up in the cathodoluminescence properties of the minerals: whereas the matrix calcite shows strong orange luminescence (normal for Fen søvites), the luminescence of the metasomatic zones is less intense, whereas the ferrocarbonatite veins themselves are non-luminescent. The C_3 metasomatism seems to have no mineralogical effects on the C_2 silicate mineral assemblage in the wall rock of the group 2 carbonatites.

C_4: *contact metasomatism associated with group 4 carbonatite.* In the composite pyroclastic

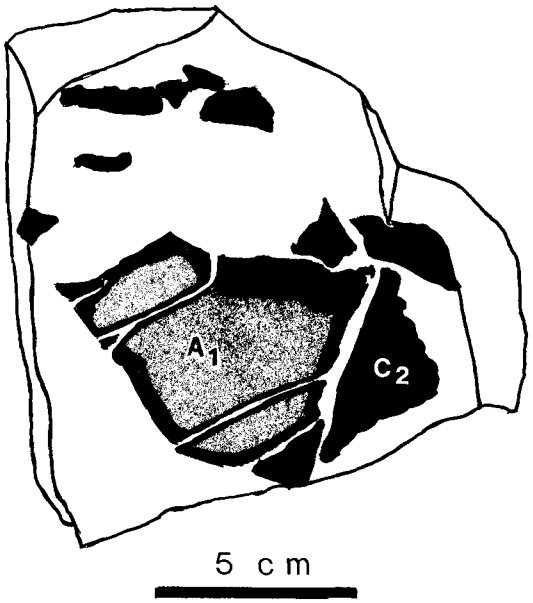

FIG. 3. The effect of C_2 contact metasomatism on feldspathic A_1 aureole fenite, drawn from photograph. The figure shows a block of group 1 søvite, containing a xenolith of A_1 fenite, from the Cappelen quarry. At the contact between søvite and fenite, a reaction rim of the C_2 mineral assemblage (phlogopite + amphibole, *black*) has formed at the expense of alkali feldspar + sodic clinopyroxene (*shaded*). The søvite is an equivalent to sample C 5.

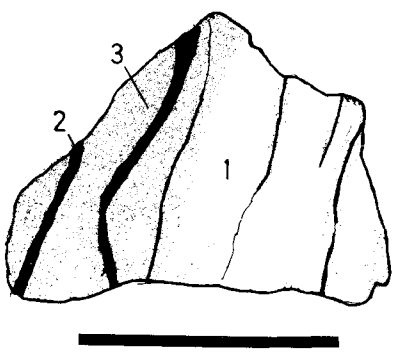

FIG. 4. The effect of C_3 contact metasomatism on søvite, drawn from a rock slab (sample C 10 from the Cappelen quarry). Numbers refer to carbonate analyses in Table 7. The black veins consist of ferrocarbonatite; the white areas represent unaffected søvite. The grey zones are recrystallized and discoloured, and show reduced cathodoluminescence intensity. Length of scale bar: 5 cm.

intrusion making up the eastern part of the Fen complex, fragments of different wallrocks are intermixed with magmatic material of ferrocarbonatite and mafic silicate composition (Andersen and Qvale, 1986). Most gneiss fragments have been transformed to chlorite + quartz + albite, but it is commonly not easy to distinguish between the effects of magmatic fluids and post-magmatic re-equilibration within this intrusion (Andersen and Qvale, 1986; Andersen, 1987*b*), nor is it always possible to identify the origin of the silicate rock fragments in the intrusion. However, in the contact zone of the intrusion at Torsnes (Fig. 1) an exposure of cross-cutting contact to a group 2 dolomite carbonatite dyke can be observed. Since this rock has not been physically incorporated into the fluidized magma, primary textures can still be discerned (Fig. 5).

This carbonatite dyke has contained phlogopite phenocrysts set in a dolomitic matrix. The phenocrysts have been transformed to chlorite, which is olive green and transparent along the rims, and brownish and cloudy in central parts of the crystals. The crystals have partly disjoined along the basal cleavage, where lamellae of calcite have been formed (Fig. 5).

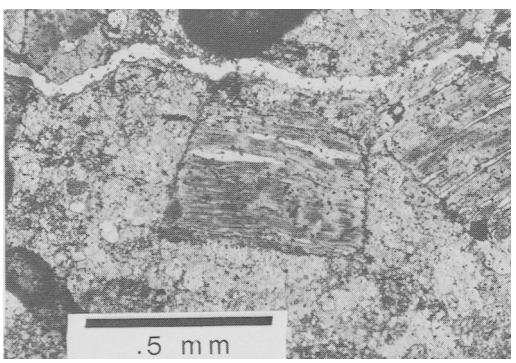

FIG. 5. The result of pseudomorphic replacement of a phlogopite phenocryst in dolomite carbonatite (group 2) with chlorite + calcite + quartz, as an effect of C_4 contact metasomatism. Sample To-2 from Torsnes.

Chronology of metasomatic events

When related to published data on the Fen intrusive and metasomatic rocks (Sæther, 1957; Andersen, 1984; Andersen and Qvale, 1986), the present observations allow a relative chronology for the different magmatic, aureole (A), and contact (C) metasomatic events in the complex to be worked out.

It is clear from structures such as illustrated in Fig. 2 that the C_1 contact metasomatism postdates the A_1 aureole fenitization. From cross-cutting relationships, the group 2 and 3 carbonatites have been interpreted as younger than the group 1 pyroxene søvite and its associated rocks (Sæther, 1957). The C_2 contact metasomatism can accordingly be interpreted as younger than both A_1 and C_1 metasomatic events, although C_1 and C_2 affect rocks in geographically separated areas. The presence of secondary stilpnomelane in group 2 carbonatites suggests that the A_2 aureole metasomatism occurred after the emplacement and solidification of these carbonatites. If so, A_2 postdates the C_2 event. The C_3 contact metasomatism affects pre-existing group 2 carbonatites, and must thus postdate C_2. Its temporal relationship to A_2 cannot be determined. The group 4 heterogeneous ferrocarbonatite cross-cut intrusive rocks of the type allied to the C_2 metasomatism, and thus the C_4 metasomatic event postdates C_2, and possibly also C_3 and A_2. A_3 (postmagmatic oxidation) is the only post-C_4 metasomatic event recorded in the Fen complex.

Mineral chemistry

Analytical methods

Pyroxenes, amphiboles, micas and most carbonates were analysed with an ARL-EMX electron microprobe, equipped with a LINK energy dispersive analyser. Standard operating conditions were: 15 kV acceleration voltage, 1 nA beam current and 100 seconds counting time. The raw-data were reduced on-line, using the commercial ZAF4/FLS computer program (Statham, 1976). Chlorites and the carbonates in sample To-2 have been analysed with a fully automatic Cameca CAMEBAX wavelength-dispersive electron microprobe (15 kV, 10 nA), using on-line PAP corrections. Both of these procedures allowed the simultaneous quantitative analysis of up to 14 elements. The microprobes were calibrated using a series of natural and synthetic mineral standards. Structural formulae were calculated on the basis of fixed numbers of cations, in the case of pyroxenes and chlorites, Fe^{3+} was estimated assuming charge balance to fixed numbers of oxygen anions. Use of a calculated Fe^{3+}/Fe^{2+} ratio can induce an error in the $Fe^{2+}/(Fe^{2+} + Mg)$ ratio, because it is influenced by analytical error in SiO_2. From repeated analyses on a series of natural and synthetic standards, a maximum analytical error of ± 1.0 wt.% absolute (2σ-values) in SiO_2 is expected in an energy dispersive analysis. This will propagate to an error of ± 7–8% in the calculated atomic $Fe^{2+}/(Fe^{2+} + Mg)$ ratio for a clinopyroxene. The corresponding error in a wavelength-dispersive analysis is significantly less.

Results

Pyroxene. Pyroxene analyses from A_1 fenite matrix and the C_1 contact metasomatic zones adjacent to pyroxene søvite are plotted in Fig. 6, selected analyses are given in Table 3.

The groundmass pyroxenes are aegirine-augites, similar to pyroxenes from fenites analysed by Kresten and Morogan (1986). In the Di–Hd–Ac (Mg–Fe^{2+} + Mn–Na) diagram, the fenite pyroxenes range from *ca.* $Di_{15}Hd_{50}Ac_{35}$ to *ca.* $Di_{10}Hd_5Ac_{85}$, similar to the variation reported from fenites by Kresten and Morogan (1986), but some grains show erratic core-to-rim zonation patterns (Fig. 6). The pale pyroxene at the interface to the carbonatite is characterized by $Ac_{>93}$, and contains only negligible Fe^{2+}, which may be the cause of the weak colour and the lack of pleochroism.

Mica. The analysed micas (Fig. 7, Table 4) fall in two different groups. The pyroxene søvite and the A_1 aureole fenite carry green biotite as a secondary phase, replacing pyroxene. This biotite is iron-rich, with annite contents above 50 mole percent, and contains appreciable octahedral aluminium (Fig. 7).

The group 2 carbonatites contain phlogopite, with *mg*-values [i.e. atomic Mg/(Mg + Fe)] corresponding to the *mg* of dolomite in the same rocks ($\geqslant$75, Table 1 in Andersen, 1986). Zoning of individual grains is oscillatory, but confined within narrow limits of *mg* (Table 4, analyses 10 and 11). The majority of analyses plot close to the phlogopite–annite join, with low tetrahedral iron, unlike phlogopites from some other carbonatites, which tend to have appreciable tetrahedral Fe^{3+} (Secher and Larsen, 1980; their Sarfartôq trend has been indicated by a broken arrow in Fig. 7). The apatite-rich rocks associated with group 2 carbonatites have phlogopites of similar composition, but with a somewhat wider variation in *mg*. The mica dominating the C_2 contact metasomatic zones is also a phlogopite, indistinguishable in composition from that of the associated carbonatites.

Amphibole. The amphiboles in group 2 carbonatites (Table 5, Figs 7 and 8) are richteritic with $(Na + K)_A > 0.5$, whereas the amphibole of undisturbed A_1 aureole fenite range towards arfedsonite and, possibly, to riebeckite and eckermannite with $(Na + K)_A < 0.5$ (Kresten and Morogan, 1986). In the C_2 contact metasomatic zones, the amphiboles range from richterite to magnesio-arfvedsonite, all with $(Na + K)_A > 0.5$.

Table 3. Pyroxene compositions

	U 1		U 6							U 6 Matrix	
	A_1 fenite		C_1 contact fenite							A_1 fenite	
	Core	Rim	Green core			Pale rim		Pale grains		Rim	Core
	1	2	3	4	5	6	7	8	9	10	11
					Weight percent oxides						
SiO_2	51.35	51.67	50.64	50.87	51.20	52.66	51.02	52.58	52.41	51.64	50.13
TiO_2	0.60	1.20	0.98	0.36	0.52	1.42	0.77	1.31	1.62	1.10	0.29
Al_2O_3	0.55	0.76	0.58	0.50	0.64	0.67	0.91	0.65	0.62	0.44	1.26
Fe_2O_3	24.86	21.48	21.44	26.55	23.71	30.63	27.98	31.63	28.68	16.27	12.23
FeO	1.58	2.37	5.16	1.65	4.20	0.00	0.00	0.00	0.47	9.27	15.27
MnO	0.49	0.60	0.67	0.79	1.01	0.03	0.36	0.00	0.25	0.74	1.53
MgO	3.10	4.40	2.55	2.17	2.26	1.28	2.41	0.88	0.96	2.70	2.97
CaO	7.98	9.86	8.76	7.19	8.18	1.03	5.35	0.43	1.03	12.24	9.21
Na_2O	9.52	8.50	8.59	9.84	9.05	13.47	11.13	13.88	13.02	6.95	5.67
Sum	100.02	100.83	99.37	99.92	100.76	101.19	99.93	101.36	99.06	101.35	98.57
					Structural formulae, based on 4.000 cations and 6.000 oxygen ions						
Si	1.965	1.955	1.968	1.961	1.965	1.974	1.945	1.969	2.009	1.982	1.997
Al(IV)	0.025	0.034	0.027	0.023	0.029	0.030	0.041	0.029	0.028	0.020	0.059
Al(VI)	0.000	0.000	0.000	0.000	0.000	0.000	0.000	0.000	0.000	0.000	0.000
Ti	0.017	0.034	0.029	0.010	0.015	0.040	0.022	0.037	0.047	0.032	0.009
Fe^{3+}	0.716	0.612	0.627	0.770	0.685	0.864	0.803	0.891	0.828	0.470	0.367
Fe^{2+}	0.050	0.075	0.168	0.053	0.135	0.000	0.000	0.000	0.015	0.298	0.509
Mn	0.016	0.019	0.022	0.026	0.033	0.001	0.012	0.000	0.008	0.024	0.052
Mg	0.177	0.248	0.148	0.125	0.129	0.072	0.137	0.049	0.055	0.154	0.176
Ca	0.327	0.400	0.365	0.297	0.336	0.041	0.218	0.017	0.042	0.503	0.393
Na	0.706	0.624	0.647	0.735	0.673	0.979	0.823	1.008	0.968	0.517	0.438

With the exception of the apatite-rich rocks, whose amphiboles are more iron-rich than the associated phlogopite, there is a good correspondence between *mg* in amphibole and mica among the rock groups studied (Fig. 7). Amphiboles from the C_2 contact metasomatic zones can easily be distinguished from those of their fenite protolith in terms of *mg*-values and Na in the *B*-position (Fig. 8), the amphibole of the contact metasomatized rocks falls to the high Na_B–high *mg* side of a comparatively well-defined dividing line in a plot of $(Na)_B$ *vs. mg*.

Chlorite. Chlorite pseudomorphs after phlogopite phenocrysts in dolomite carbonatite affected by C_4 contact metasomatism (sample To-2, see Figs 7 and 9, Table 6) have low calculated Fe^{3+}, and classify as clinochlore to penninite in the nomenclature of Hey (1954). The chlorite has uniform *mg*, nearly identical to that of the phlogopite from which it has formed (Fig. 9). However, they have higher Si and Mg and lower Fe and Al than the ripidolitic to thuringitic chlorites in rødberg, formed during the A_3 post-magmatic alteration (Fig. 9; data from Andersen, 1984).

The brown, interior parts of the chlorite crystals have distinctly higher K_2O than the olive-green rims (Fig. 9). The brown parts of the crystals probably represent an intermediate stage of the alteration process, involving the progressive loss of interlayer K^+ cations. A similar evolution, but at different compositions, is seen among the chlorites formed by the alteration of metamorphic biotites in country-rock gneisses affected by the A_3 metasomatism (Andersen, 1984, plotted in Fig. 9 for comparison).

Carbonates. Carbonate compositions are plot-

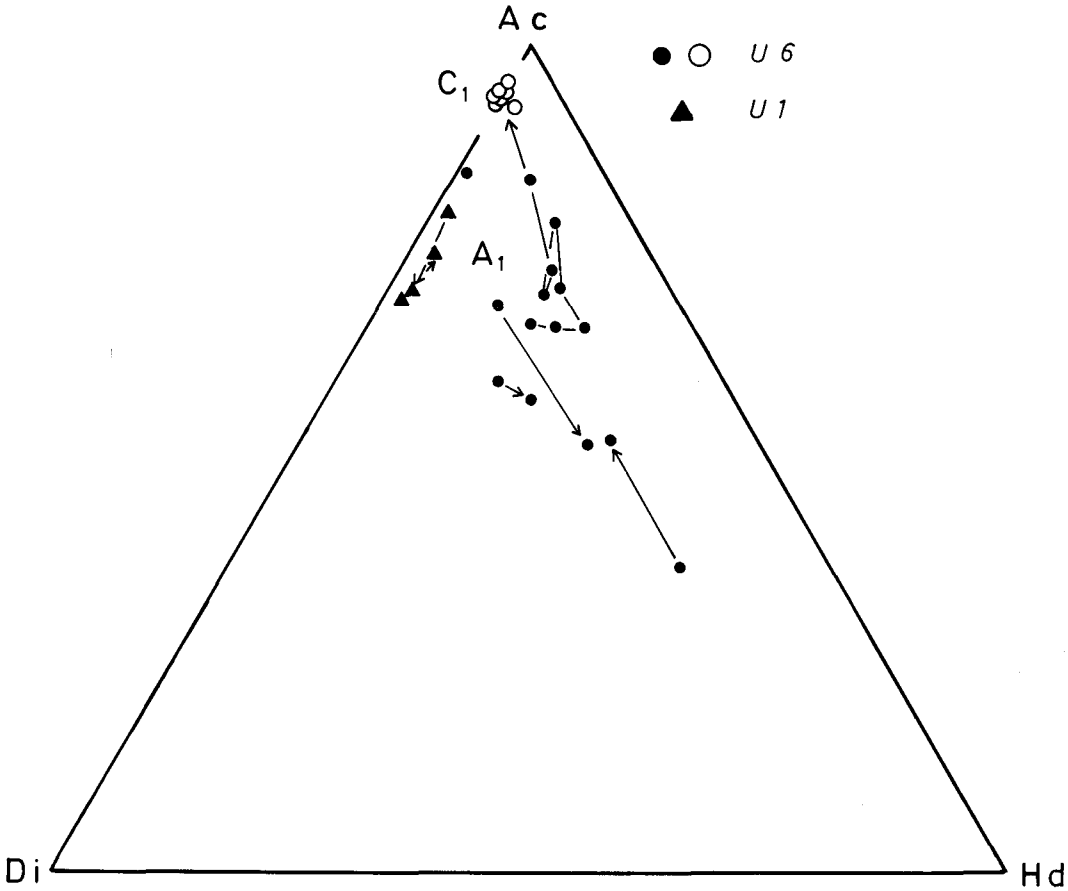

FIG. 6. Clinopyroxene analyses projected to the Di–Hd–Ac plane, represented by Mg–Fe^{2+} + Mn–Na. Solid symbols refer to A_1 minerals, the open circles to pyroxene affected by C_1 contact metasomatism. Selected microprobe analyses are given in Table 3. *Arrows:* core to rim zoning.

ted in Fig. 10 and relevant analytical data are given in Table 7.

Analyses of groundmass calcite in the søvite forming the wall-rock to dyke-facies ferrocarbonatite, show that it is very close to pure end-member composition. The carbonate of the ferrocarbonatite is an ankerite with *ca.* 40 mol percent of the $CaFe(CO_3)_2$ component, corresponding to the maximum iron content of ankerite reported from ferrocarbonatite by Andersen (1984). The recrystallized calcite of the C_3 contact metasomatic zones has significantly higher Fe, Mg, and Mn content than the matrix calcite in søvite. This change in composition correlates with the reduction of cathodoluminescence intensity observed.

Dolomite from group 2 carbonatites ranges from $CaMg_{0.75}Fe_{0.25}(CO_3)_2$ to $CaMg_{0.95}Fe_{0.05}(CO_3)_2$ (Fig. 10). The matrix dolomite of sample To-2 falls within this range, whereas the calcite formed during pseudomorphic replacement of phlogopite by chlorite in this sample is close to the pure end-member composition.

Discussion

A system consisting of an intrusive magma volume and its immediate wall-rock is in chemical and thermal disequilibrium. Even if the temperature at the interface between magma and wall-rock may rapidly rise to approach that of the magma itself, a compositional contrast will persist. Contact metasomatic processes tend to reduce the compositional gradient, by material

Table 4. Composition of micas.

	U 2	U 4	WCB 5	H 1			T 3	4/28.45	H 5	H 8		C 5
	A_1 -	Group 1 carb.		C_1 - Altered fenite				Group 2 carbonatites				
	Fenite	Pyroxene søvite						Apatite rock	Phlogopite - amphibole søvite			
	1	2	3	4	5	6	7	8	9	10	11	12
						Weight percent oxides						
SiO_2	36.18	36.09	34.57	42.72	40.82	42.31	41.08	38.15	41.69	42.26	41.85	41.29
TiO_2	0.24	4.51	3.57	0.99	1.68	1.23	1.14	0.75	0.32	0.22	0.26	0.97
Al_2O_3	17.26	13.09	12.33	12.25	11.98	11.61	10.07	12.08	12.89	12.35	12.51	11.88
FeO	23.60	22.73	30.07	4.59	10.23	6.73	11.35	14.39	3.23	3.59	3.96	9.68
MnO	0.16	0.20	0.59	0.08	0.37	0.06	0.18	0.00	0.12	0.09	0.24	0.00
MgO	8.47	10.25	5.09	25.02	20.58	23.63	21.02	17.69	26.93	26.33	22.55	21.78
CaO	0.00	0.00	0.13	0.11	0.09	0.13	0.01	0.76	0.11	0.06	0.17	0.20
Na_2O	0.35	0.46	0.07	0.17	0.21	0.18	0.10	1.82	0.46	0.64	0.50	0.16
K_2O	10.08	10.14	9.77	11.01	10.30	10.42	10.26	9.62	10.70	10.55	10.32	10.35
Sum	96.34	97.47	96.19	96.94	96.26	96.30	95.21	95.26	96.45	96.09	92.36	96.31
						Structural formulae based on 16.000 cations						
Si	5.635	5.596	5.658	6.017	5.971	6.066	6.082	5.653	5.814	5.928	6.187	5.989
Al(IV)	2.365	2.392	2.342	1.983	2.029	1.934	1.757	2.110	2.119	2.042	1.813	2.031
Al(VI)	0.803	0.000	0.037	0.051	0.036	0.028	0.000	0.000	0.000	0.000	0.366	0.000
Ti	0.028	0.526	0.439	0.105	0.185	0.133	0.127	0.084	0.034	0.023	0.029	0.106
Fe2+	3.074	2.947	4.116	0.541	1.251	0.807	1.405	1.783	0.377	0.421	0.490	1.174
Mn	0.021	0.026	0.082	0.010	0.046	0.007	0.023	0.000	0.014	0.011	0.030	0.000
Mg	1.966	2.369	1.242	5.253	4.487	5.050	4.639	3.908	5.598	5.505	4.969	4.709
Ca	0.000	0.000	0.023	0.017	0.014	0.020	0.002	0.121	0.016	0.009	0.027	0.031
Na	0.106	0.138	0.022	0.046	0.060	0.050	0.029	0.523	0.124	0.174	0.143	0.045
K	2.003	2.006	2.040	1.978	1.922	1.906	1.938	1.819	1.904	1.888	1.946	1.915
mg	39.01	44.56	23.18	90.67	78.19	86.22	76.75	68.66	93.70	92.89	91.03	80.04

transport processes across the magma to wall-rock interface.

Some of the contact metasomatic processes described from the Fen complex have affected silicate rocks or silicate minerals in carbonatites, which are less susceptible to late/post magmatic modifications than the carbonate minerals of the carbonatites. The metasomatic products in question (i.e. the C_1, C_2 and C_4 parageneses) may therefore be assumed to preserve a memory of activity relationships in the carbonatite magma, which may be lost from the carbonatites themselves. Furthermore, because the different groups of carbonatite intrusions have induced different contact metasomatic reactions in uniform wall-rocks, the reactions observed may be used as qualitative to semiquantitative guidelines to the difference in composition between the respective carbonatite magma types.

Mass balance of contact metasomatism

Material which has been added to a rock during carbonatite-induced contact metasomatism must have been derived from the carbonatite magma. Among the four distinct types of contact metasomatism recognized in Table 2, C_3 stands out as a simple case of introduction of ferromagnesian components ($FeCO_3$, $MgCO_3$ and $MnCO_3$ 'molecules') into a monomineralic calcite carbonatite. The shift of carbonate composition during C_3 metasomatism is illustrated by an arrow in Fig. 10. As can be seen, this shift goes in the general direction of the intruding carbonatite liquid represented by the ankerite of the ferrocarbonatite.

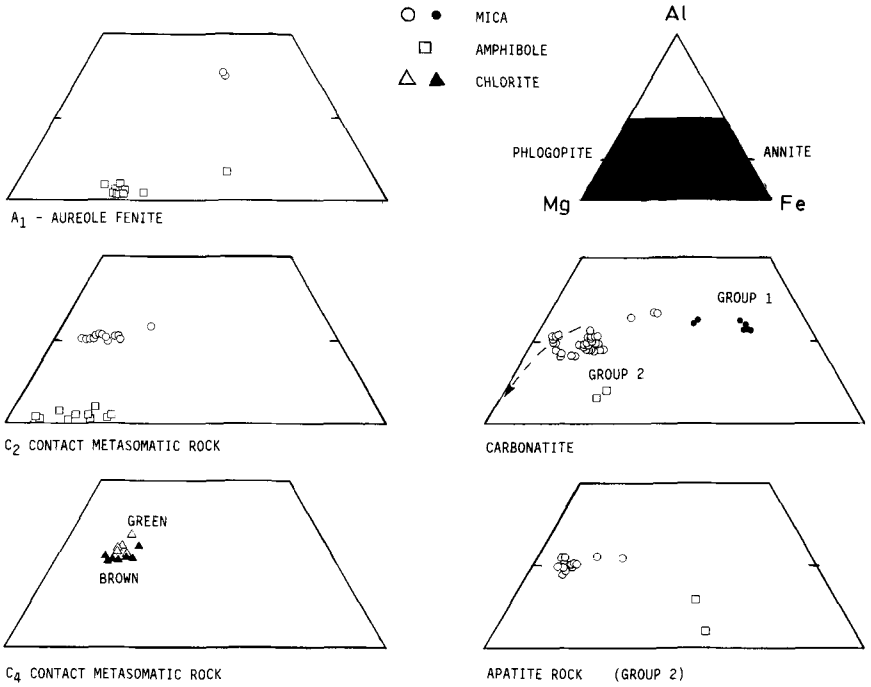

FIG. 7. Mafic aluminosilicates (mica, amphibole, chlorite) in A_1 fenite and C_2 and C_4 contact metasomatic rocks. Selected microprobe analyses are given in Tables 4, 5 and 6. Broken arrow: The evolution towards tetra-ferri phlogopite in the Sarfartôq carbonatite complex, Greenland (Secher and Larsen, 1980) shown for comparison.

The other contact metasomatic processes (C_1, C_2, C_4) are more complex, for the very reason that they act on polymineralic silicate rocks or carbonatites containing significant amounts of silicate minerals. The mass balance effects of these processes are best illustrated in an Al − Na + K − Fe^{tot} + Mg triangular diagram (Fig. 11).

C_1 and C_2 both act on A_1 aureole fenites, characterized by a perthitic alkali feldspar (or albite + microcline; Kresten and Morogan, 1986), aegirine-augite (CPX1) and an alkali amphibole with variable *mg* (AMPH1) (Fig. 11). Regardless of the actual modal feldspar to mafic silicate ratio, the strongly peralkaline pyroxene and amphibole minerals make the A_1 fenites peralkaline rocks with agpaitic indexes (atomic (Na + K)/Al) > 1.0.

During the C_1 contact metasomatism, pyroxene and feldspar(s) remain stable as phases, but change in composition. The shift in K-feldspar composition from $Or_{>90}$ to Or_{75} may be a thermal effect rather than a result of metasomatic introduction of sodium, whereas the change in pyroxene composition (CPX1 to CPX2 in Fig. 11) can be described as an exchange of pyroxene components between melt and pyroxene:

$$Ca(Mg,Fe)Si_2O_{6cpx} + [NaFeSi_2O_6]_{melt} = [Ca(Mg,Fe)Si_2O_6]_{melt} + NaFeSi_2O_{6cpx}.$$

Because the loss of Mg from the pyroxene is compensated by a gain in ferric iron, the shift in pyroxene composition is constrained to a straight line at constant (Fe^{tot} + Mg)/Al towards the Na + K apex in the projection of Fig. 11. In this process, the agpaitic index of the system of course increases.

The main modal effect of the C_2 metasomatism is replacement of the feldspar phase(s) of the A_1 fenite by phlogopite. Compared to the mafic silicates of the A_1 paragenesis, the C_2 phlogopite has much higher *mg* (Fig. 7), suggesting that the total C_2 process may be adequately described as a case of magnesium metasomatism. In this process amphibole remained stable, only shifting slightly in direction away from the Na + K apex (AMPH1 to AMPH2 in Fig. 11), and towards higher *mg* (Fig. 8). Because of the high (Na + K)/Al ratio of the amphibole, the bulk rock has remained peralkaline through this alteration process; the agpaitic index may, however, have stayed constant or shifted slightly in either direction (Fig. 11).

Table 5. Compositions of amphiboles

	H4	H4	H4	H4	T3	H1	H1	C5	4/28.45
	Fenite relict, Hydro quarry				Altered fenite			Søvite	Apatite rock
		Core	Rim						
	1	2	3	4	5	6	7	8	9
					Weight percent oxides				
SiO_2	55.79	54.83	55.02	56.34	55.24	56.84	57.74	51.72	52.02
TiO_2	0.45	0.82	0.76	0.05	0.24	0.35	0.34	0.98	0.40
Al_2O_3	2.33	1.71	1.48	0.39	0.45	0.25	0.23	3.16	1.31
FeO	21.65	9.28	11.06	12.50	10.46	6.78	3.18	11.74	23.13
MnO	0.13	0.51	0.67	0.04	0.09	0.21	0.04	0.23	0.00
MgO	8.72	17.70	16.79	16.95	17.46	20.25	22.12	15.83	9.53
CaO	0.60	4.76	3.32	0.57	1.69	4.02	6.51	5.68	1.57
Na_2O	7.70	6.15	6.69	7.80	8.01	6.34	5.94	6.19	7.76
K_2O	0.00	1.54	1.72	2.30	1.90	1.30	1.40	1.61	0.01
Sum	97.37	97.30	97.51	96.94	95.54	96.34	97.50	97.14	95.73
			Structural formulae, based on Si+Al+Ti+Mn+Mg = 13.000						
Si	8.051	7.745	7.759	7.910	7.909	7.909	7.991	7.488	7.736
Al(IV)	0.000	0.255	0.241	0.065	0.076	0.041	0.009	0.512	0.230
Al(VI)	0.396	0.029	0.005	0.000	0.000	0.000	0.029	0.027	0.000
Ti	0.049	0.087	0.081	0.005	0.026	0.037	0.035	0.107	0.045
Fe2+	2.613	1.096	1.304	1.468	1.252	0.789	0.368	1.421	2.877
Mn	0.016	0.061	0.080	0.005	0.011	0.025	0.005	0.028	0.000
Mg	1.876	3.727	3.530	3.547	3.726	4.200	4.563	3.416	2.113
Ca	0.093	0.720	0.502	0.086	0.259	0.599	0.965	0.881	0.250
Na	2.154	1.684	1.829	2.123	2.223	1.710	1.594	1.738	2.238
K	0.000	0.277	0.309	0.412	0.347	0.231	0.247	0.297	0.002
SUM:	15.25	15.68	15.64	15.62	15.83	15.54	15.81	15.92	15.49
(Na+K)A	0.25	0.68	0.64	0.62	0.83	0.54	0.81	0.92	0.49
(Na)B	1.91	1.28	1.50	1.91	1.74	1.40	1.03	1.12	1.75

The C_4 process involves the pseudomorphic replacement of phlogopite phenocrysts in group 2 dolomite carbonatite by chlorite + calcite + quartz, while the matrix dolomite has remained stable. The replacement of phlogopite by a silica-rich chlorite and calcite in the presence of dolomite is described by the reaction:

$$6\text{phl} + 3\text{dol} + 8H_2O = \text{chl} + \text{qz} + 3\text{cc} + 6K^+ + 3CO_3^{2-}$$

where

$$\text{chl} = 3Mg_5AlAlSi_3O_{10}(OH)_8 - 2Mg_3Si_4O_{10}(OH)_2,$$

i.e. a siliceous chlorite (penninite) intermediate between the clinochlore and talc–chlorite end-members. This suggests that the C_4 process may be adequately described by hydration and leaching of alkalis and CO_2 from the rock. In the coordinates of Fig. 11 this evolution is represented by a shift from an alkaline mineral assemblage (phlogopite + dolomite, agpaitic index = 1) to a clearly subalkaline paragenesis (chlorite + dolomite, agpaitic index $\ll 1$). At its extreme (olive green chlorite), the C_4 mineral assemblage in the altered dolomite carbonatite is alkali-free (tie-line C_4^F in Fig. 11); the brown chlorite represents intermediate stages of a progressive alkali leaching process (tie line C_4^I in Fig. 11).

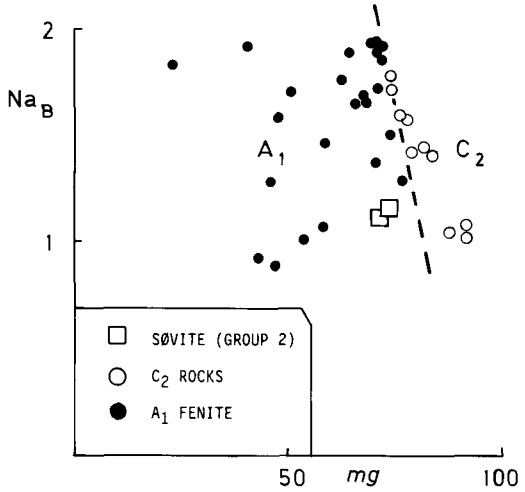

FIG. 8. Characteristics of amphiboles in A_1 fenite and C_2 contact metasomatic rocks, Na in the B-position *vs.* *mg* = atomic Mg/(Mg + Fe). The broken line separates the C_2 contact metasomatic amphiboles from those of the A_1 aureole fenite.

Contact metasomatism and carbonatite magmas

Simple qualitative or semiquantitative bulk composition considerations, such as presented above, suggest the presence of carbonatite magmas of different compositional character in the Fen complex. The melts responsible for C_1 must have been distinctly peralkaline, in order to increase the agpaitic index of the wall-rock, whereas the source of the C_4 metasomatism must have been clearly subalkaline, to allow alkali depletion in their wall-rock. In order to be more specific, it is necessary to discuss the carbonatite magmas in terms of the activities of their major components.

A carbonatite magma may be regarded as an ionic melt consisting of metal carbonate components (Treiman and Schedl, 1983). The Fen carbonatites today contain calcite, dolomite and dolomite–ferrodolomite solid solution, but the presence of smaller or larger amounts of alkali components in the melt cannot be ruled out *a priori*. It is therefore most convenient to discuss the magmas in terms of the components $CaCO_3$, $MgCO_3$, $FeCO_3$, Na_2CO_3 and K_2CO_3. In the C_2 and C_4 contact metasomatic processes mafic aluminosilicates (phlogopite and chlorite), alkali feldspar, quartz and a fluid phase also take part. This introduces Al_2O_3, SiO_2, H_2O and CO_2 as additional components necessary to describe the total system.

As long as only processes taking place at the contact surface of the intrusions themselves are concerned, the system can be assumed to be isobaric, and the temperature of metasomatism may be taken as constant and set equal to the temperature of the magma, which is in the range 625–650 °C for carbonatite magmas crystallizing calcite in the presence of an aqueous fluid phase (Wyllie, 1966).

In the absence of thermodynamical data on molten metal carbonates, the relationship between component activities in a carbonatite magma and contact metasomatic mineral reactions is best illustrated in isothermal, uncalibrated orthogonal log activity diagrams (Fig. 12). In such diagrams, equilibrium phase assemblages are located on straight lines whose slopes are given by the stoichiometric coefficients of the components in the corresponding reactions.

The mineral reactions involved in the C_2 and C_4 processes are listed in Table 8, together with their equilibrium constant expressions, assuming (1) that the mafic silicate minerals are present as pure magnesium end-members, and (2) that the $CaCO_3$-activity is buffered by solid calcite. The mafic silicates formed during C_2 and C_4 metasomatism have high and uniform *mg*-values, suggesting that it is permissible to disregard the $FeCO_3$ component in the carbonatite melt in the discussion. The second assumption rests on the observation that calcite is omnipresent in these rocks, either as the major liquidus phase of the carbonatite magma, or as a mineral forming during contact metasomatism. Some of the reactions in Table 8 are dependent on the composition of the fluid phase. Experimental data show that carbonatite magmas are only stable at reasonable temperatures in the presence of a water-dominated binary H_2O–CO_2 fluid phase (Wyllie, 1966). The presence of such a fluid phase during crystallization of carbonatite magma at Fen is documented by water-rich fluid inclusions in liquidus apatite (Andersen, 1986). The composition of the fluid phase present during contact metasomatism can therefore be assumed to have been controlled by the carbonatite magma itself, rather than by reactions involving the wall-rocks, at approximately constant $X_{CO_2} \ll X_{H_2O}$.

Fig. 12 has been constructed assuming that K-feldspar and dolomite are not stable together as liquidus minerals in the carbonatite. The reaction Kf + 3Dol + H_2O = Phl + 3Cc + $3CO_2$ defines the high-temperature stability limit of the K-feldspar + dolomite paragenesis. At shallow crustal pressures (1–2 kbars) and realistic carbonatite magma temperature (625–650 °C) this reaction is widely overstepped for any fluid phase composition compatible with a carbonatite magma

Table 6. Chlorite compositions

	To 2 Contact metasomatized dolomite carbonatite, Torsnes						
	Grain 1 Green 1	Brown 2	Brown 3	Brown 4	Green 5	Grain 2 Brown 6	Green 7
	Weight percent oxides						
SiO_2	31.48	35.82	34.08	34.71	31.81	32.03	30.39
TiO_2	0.09	0.70	1.98	0.52	0.70	0.99	0.03
Al_2O_3	17.21	14.33	14.51	14.49	15.59	15.34	17.27
FeO	12.91	11.46	12.80	11.43	14.00	14.37	12.27
MnO	0.10	0.13	0.17	0.23	0.18	0.31	0.05
MgO	25.61	24.80	24.60	24.81	23.47	24.00	25.92
CaO	0.18	0.08	0.03	0.11	0.00	0.06	0.13
Na_2O	0.05	0.05	0.10	0.64	0.05	0.00	0.03
K_2O	0.24	2.99	2.33	3.03	1.16	1.41	0.33
Sum	87.88	90.35	90.61	89.97	86.96	88.50	86.40
	Structural formulae, based on 20.000 cations and 28.000 oxygen ions						
Si	6.204	6.896	6.593	6.666	6.418	6.357	6.059
Al(IV)	1.796	1.104	1.407	1.334	1.582	1.643	1.941
Al(VI)	2.201	2.148	1.901	1.946	2.125	1.947	2.117
Ti	0.013	0.101	0.287	0.074	0.106	0.147	0.005
Fe3+				0.221			
Fe2+	2.127	1.844	2.071	1.615	2.361	2.386	2.046
Mn	0.017	0.021	0.029	0.037	0.031	0.052	0.008
Mg	7.523	7.118	7.094	7.102	7.058	7.100	7.704
Ca	0.038	0.017	0.006	0.023	0.000	0.012	0.028
Na	0.019	0.019	0.039	0.238	0.020	0.000	0.010
K	0.061	0.733	0.574	0.743	0.299	0.356	0.083
Charge	56.35	56.49	56.46	56.00	56.44	56.24	56.09

Table 7. Compositions of carbonates

	C 10			To 2 Dolomite carbonatite	
	Søvite matrix	F.C. vein	Altered zone	Matrix	Lamellae in Chl
	1	2	3	4	5
	Weight percent oxides				
FeO	0.35	14.97	1.62	3.63	0.39
MnO	0.00	2.27	0.36	1.57	0.73
MgO	0.21	10.25	1.35	18.84	0.02
CaO	54.66	27.08	52.12	30.38	54.85
Sum	55.22	54.57	55.45	54.42	55.99
	Structural formulae based on 2.000 cations				
Fe	0.010	0.426	0.046	0.093	0.015
Mn	0.000	0.065	0.010	0.041	0.028
Mg	0.011	0.520	0.068	0.864	0.001
Ca	1.980	0.988	1.877	1.002	1.956

Analyses 1-3 were made with an ARL-EMX microprobe equipped with a LINK energy dispersive analyser, analyses 4-5 were made using a CAMEBAX wavelength-dispersive electron microprobe.

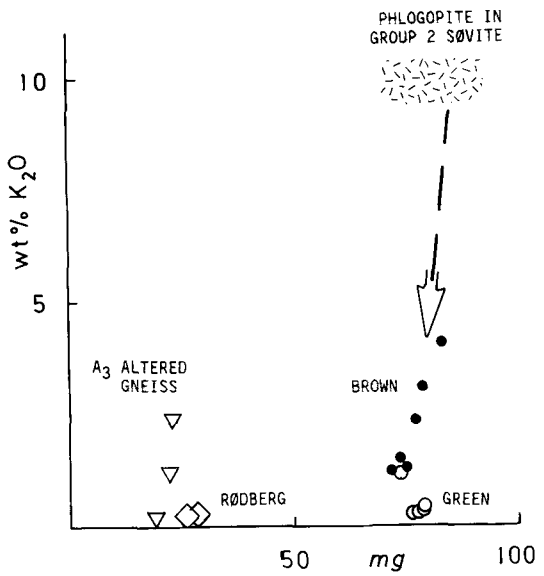

FIG. 9. Chemical evolution of C_4 chlorite: wt. % K_2O *vs. mg*. The data for A_3 rocks (altered gneiss and rødberg, i.e. hematite carbonatite) were taken from Andersen (1984).

Table 8. Reactions describing contact metasomatic alteration of aluminosilicate minerals during C_2 and C_4 contact metasomatism.

(1) $Kf + 3\,[MgCO_3] + H_2O = Phl + 3\,CO_2$
$\log K_1 = 3 \log a_{CO2} - 3 \log a_{MgCO3} - \log a_{H2O}$

(2) $6\,Phl + 3\,[MgCO_3] + 8\,H_2O = Chl + Qz + 3\,[K_2CO_3]$
$\log K_2 = 3 \log a_{K2CO3} - 3 \log a_{MgCO3} - 8 \log a_{H2O}$

(3) $6\,Kf + 21\,[MgCO_3] + 14\,H_2O = Chl + Qz + 3\,[K_2CO_3] + 18\,CO_2$
$\log K_3 = 3 \log a_{K2CO3} + 18 \log a_{CO2} - 21 \log a_{MgCO3} - 14 \log a_{H2O}$

(4) $2\,Ab + [K_2CO_3] = 2\,Kf + [Na_2CO_3]$
$\log K_4 = \log a_{Na2CO3} - \log a_{K2CO3}$

(5) $2\,Ab + [K_2CO_3] + 6\,[MgCO_3] + 2\,H_2O = 2\,Phl + [Na_2CO_3] + 6\,CO_2$
$\log K_5 = \log a_{Na2CO3} + 6 \log a_{CO2} - 6 \log a_{MgCO3} - \log a_{K2CO3} - 2 \log a_{H2O}$

(6) $6\,Ab + 21\,[MgCO_3] + 14\,H_2O = Chl + Qz + 3\,[Na_2CO_3] + 18\,CO_2$
$\log K_6 = 3 \log a_{Na2CO3} + 18 \log a_{CO2} - 21 \log a_{MgCO3} - 14 \log a_{H2O}$

(7) $Cc + [MgCO_3] = Dol$
$\log K_7 = - \log a_{MgCO3}$

(8) $Cc + [K_2CO_3] = Fc$
$\log K_8 = - \log a_{K2CO3}$

Kf = K-feldspar, Ab = albite, Qz = quartz, Phl = phlogopite, Chl = $(3Mg_5AlAlSi_3O_{10}(OH)_8 \cdot 2Mg_3Si_4O_{10}(OH)_2)$, i.e. a siliceous chlorite (penninite) intermediate between the chlinochlore and talk-chlorite endmembers, Cc = calcite, Dol = Dolomite, Fc = Fairchildite $(K_2Ca(CO_3)_3)$.

(Greenwood, 1976; Rice, 1977; Wyllie, 1966). This is, however, based on the assumption of excess calcite, and does not contradict the existence of K-feldspar + dolomite-bearing carbonatites without primary calcite, such as the

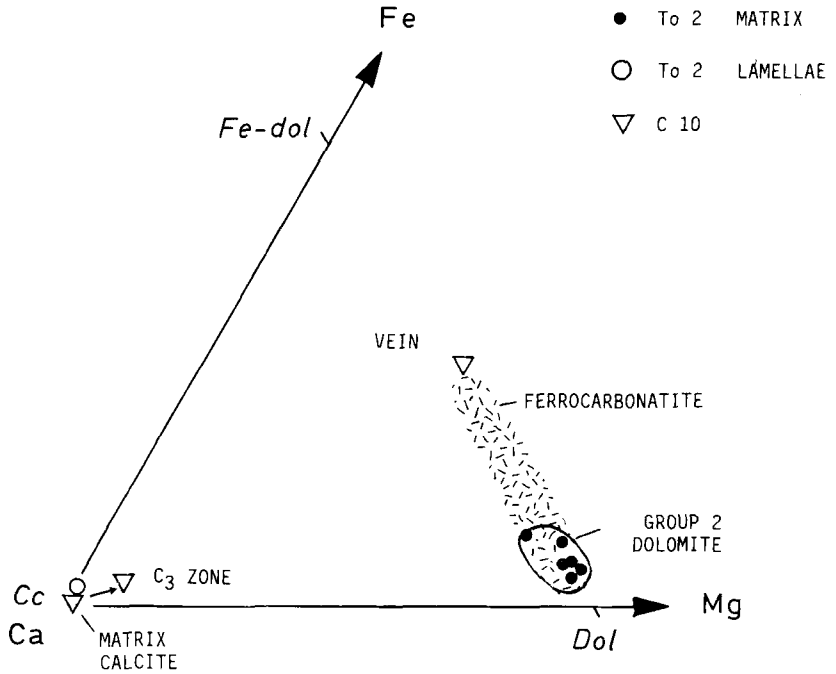

FIG. 10. Carbonates in group 3 ferrocarbonatite, group 2 carbonatites and C_3 contact metasomatic rocks. Ranges of variation of dolomites in group 2 carbonatites and in ferrocarbonatites (groups 3 and 4) are also indicated. The shift of calcite compositions during C_3 contact metasomatism is shown as an arrow.

beforsites from Alnö (v. Eckermann, 1948; Kresten, 1979).

In the sodium-free model carbonatite system ($CaCO_3-MgCO_3-K_2CO_3-SiO_2-Al_2O_3-H_2O-CO_2$) the seven-phase assemblage Kf + Phl + Chl + Qz + Cc + l + v is invariant at constant *P* and *T*. (I in the isobaric–isothermal log $a_{K_2CO_3}$ *vs.* log a_{MgCO_3} diagram, Fig. 12). Among the several possible univariant mineral reactions in this assemblage, reactions 1, 2 and 3 in Table 8 relate the contact-metasomatic processes observed at Fen to the activity relationships in the carbonatite magmas. The presence of sodium in the system may lead to the stabilization of albite as a phase, related to the other minerals by reactions 4 to 6 in Table 8. In Fig. 12, the stability field of albite is projected to the log $a_{K_2CO_3}$ *vs.* log a_{MgCO_3} plane from two different levels of Na_2CO_3 activity. The saturation limits of dolomite and an alkali carbonate mineral (nyerereite–fairchildite solid solution: $(Na,K)_2Ca(CO_3)_3$) are also indicated in the diagram.

Since the A_1 and C_1 parageneses are identical in this simplified system (Ab + Kf + sodic Cpx/Amph), the $MgCO_3$–K_2CO_3 activity diagram does not distinguish between the activity conditions of the A_1 protolith and the product of C_1 contact metasomatism. However, the A_1 and C_1 mineral assemblages suggests that both processes took place at low $MgCO_3$ activity, but at comparatively high K_2CO_3 and Na_2CO_3 activity levels (Fig. 12*b*). The C_2 process, on the other hand, has involved an increase in $MgCO_3$ activity, sufficient to change from an A_1-protolith into the field of phlogopite stability. The behaviour of the K_2CO_3 and Na_2CO_3 activities during this process cannot be deduced with certainty, but the non-existence of carbonatites or contact metasomatic rocks with the equilibrium mineral assemblages Phl + Ab seems to suggest a drop in at least $a_{Na_2CO_3}$, probably also in $a_{K_2CO_3}$ relative to that of the A_1 fenite precursor (Fig. 12*b*).

A drastic drop in K_2CO_3 activity is, however, indicated during the C_4 metasomatic process. This takes place wholly within the field of dolomite stability; the system moves from the Phl + Dol field of the group 2 carbonatite protolith, into the Chl + Dol field (Fig. 12*b*). Under these conditions, reaction 2 in Table 8 becomes an equivalent to the hydration and leaching-reaction derived for C_4 metasomatism above.

From a physicochemical point of view, gradi-

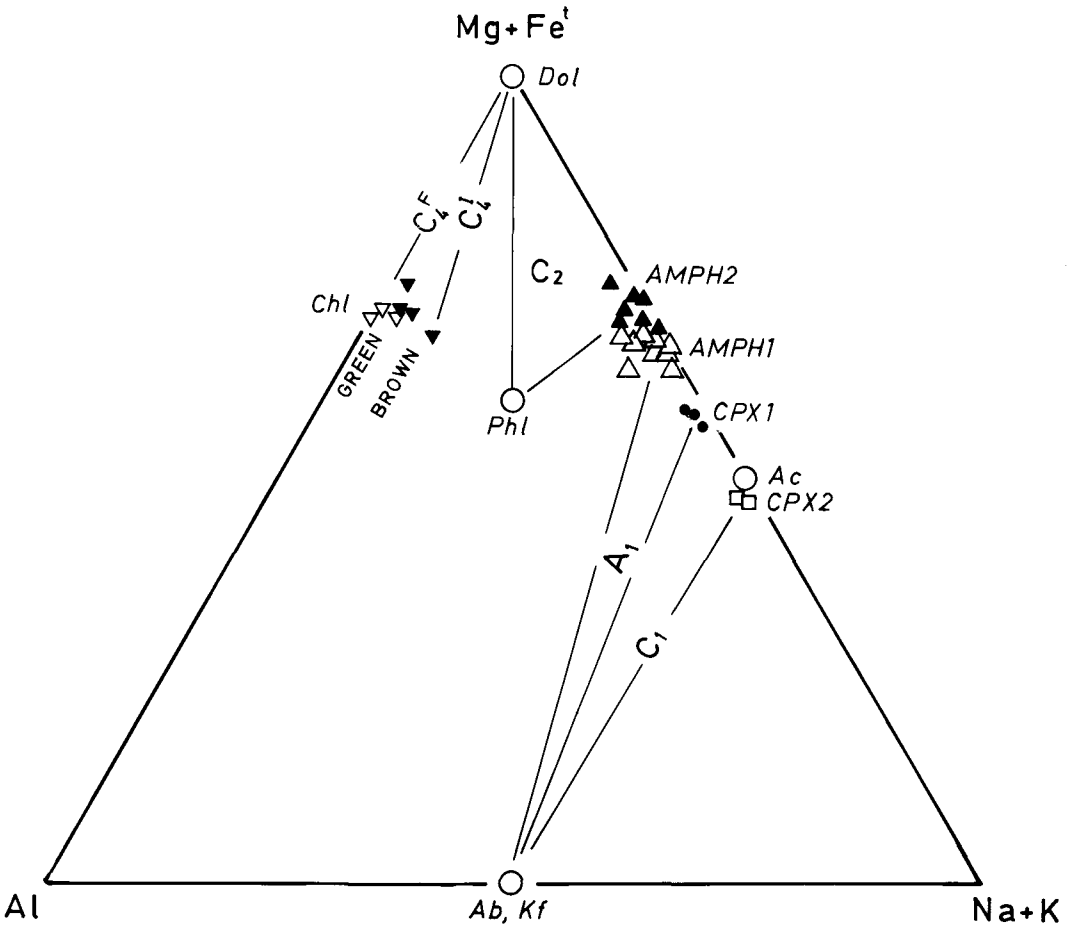

FIG. 11. Mass balance of contact metasomatism, illustrated in the atomic Al–(Fe + Mg)–(Na + K) diagram. CPX1: Clinopyroxene (aegirine augite) of the A_1 aureole fenite assemblage. CPX2: Clinopyroxene (aegirine) of the C_1 contact metasomatic mineral assemblage. AMPH1: Amphibole in A_1 fenite. AMPH2: Amphibole of C_2 contact metasomatic rocks. The positions of different aureole- and contact metasomatic rock systems in the diagram are indicated. (See discussion in the text.)

ents in chemical potential of components constitute the driving force behind the material transport processes seen in contact metasomatism. The chemical potential of a component i is related to the activity of the component by the expression $\mu_i = \mu_i^0 + RT \ln a_i$, where μ_i is the chemical potential, μ_i^0 is the chemical potential of the pure component in its standard state, and a_i is its activity (e.g. Castellan, 1971). The changes in activity of either of the components during contact metasomatism derived from Fig. 12 must therefore point in the direction of the activity conditions of the magma causing the contact metasomatism. Fig. 12*b* illustrates the characteristics of the three different carbonatite magma types which have induced the C_1, C_2 and C_4 contact metasomatic processes as derived from the above considerations.

The carbonatite magmas forming group 1 pyroxene søvite/silicosøvite were characterized by low $MgCO_3$ activity and high alkali carbonate activities. There are, however, no petrographic indications of the earlier presence of alkali carbonate minerals in these carbonatites (Andersen, 1988), nor have such minerals been formed in the C_1 metasomatic zones. This suggests that the stability limit of nyerereite–fairchildite s.s. was never overstepped by these carbonatite magmas, and

supports the conclusion of Andersen (1988) that the pyroxene søvite intrusions crystallized from 'peralkaline calcite carbonatite magmas'. Again, it should be noted that the activity conditions of the A_1 protolith and the C_1 metasomatic mineral assemblage are indistinguishable in this projection, hence the group 1 magma-field will overlap with the protolith/C_1 field in Fig. 12*b*. The group 2 (and group 3) carbonatite magmas have induced a shift towards higher a_{MgCO_3} and (possibly) lower $a_{K_2CO_3}$, from an A_1 protolith. The magma field must therefore be situated to the high a_{MgCO_3}–low $a_{K_2CO_3}$ side of the C_2 field in the diagram. Among these carbonatites, the dolomite carbonatites must have crystallized from magmas with higher $MgCO_3$ activity. The topology of the diagram also suggests a higher relative level of $a_{K_2CO_3}$ in the dolomite carbonatite magmas (Fig. 12*b*). Resorbed dolomite crystals in some group 2 søvites suggest that some batches of calcite carbonatite magma have evolved from dolomite-saturation to undersaturation at some stage of their crystallization history. The carbonatite magmas involved in C_2 metasomatism have lost part of their Mg-content in order to transform feldspar to phlogopite along the intrusive contact. In some, initially dolomite-saturated calcite carbonatite magmas, this Mg-loss may have been sufficient to destabilize dolomite as a liquidus phase.

The low *mg*-value of the primary carbonates of ferrocarbonatite imply that these rocks formed from magmas characterized by an elevated a_{FeCO_3}, which makes Fig. 12 incomplete as a representation of these melts. However, the absence of reactions between group 3 ferrocarbonatite intrusions and the C_2 silicate mineral assemblage suggests that the magma forming these dykes and veins would have magnesium and alkali carbonate activity levels comparable to those of the group 2 dolomite carbonatite magma.

To induce a shift from group 2 dolomite carbonatite conditions into the C_4-field, the group 4 ferrocarbonatite magma must have been characterized by a low level of K_2CO_3-activity compared to other carbonatite magmas at Fen (Fig. 12*b*). The intimate association of this ferrocarbonatite with mafic silicate rocks related to damtjernite (Andersen and Qvale, 1986) suggests a close genetic relationship between these two rock-types, most probably by liquid immiscibility at a shallow level in the crust (cf. Hay, 1978; Treiman and Essene, 1985). Recent experimental findings suggest that the pertinent carbonatite + silicate two-liquid field extends to alkali-free, Ca–Mg–Fe-dominated carbonatite compositions, which would be equivalent to the Fen group 4 ferrocarbonatite (Kjarsgaard and Hamilton, 1988).

Implications

Several recent studies have demonstrated the importance of liquid immiscibility, fractional crystallization and wall-rock contamination processes for the evolution of carbonatite magma in the Fen complex (e.g. Mitchell and Brunfelt, 1975; Andersen 1987*a*; Andersen and Sundvoll, 1987; Andersen and Taylor, 1988). The present results suggest that group 3 ferrocarbonatite and group 2 søvite/dolomite carbonatite have comparable $MgCO_3$ and K_2CO_3 activity levels; these carbonatite groups are also indistinguishable in trace element and isotopic compositions (Andersen, 1987*a*; see Table 1, above). These findings may imply that these two groups of carbonatites are cogenetic. On the other hand, neither the peralkaline calcite carbonatite magma forming the group 1 pyroxene søvite/silicosøvite, nor the group 4 ferrocarbonatite magma have component activity characteristics compatible with a status as derivatives or precursors for any of the other carbonatite magmas which evolved in the Fen complex. Both geological observations and geochemical and mineralogical data suggest that these carbonatites are the products of local trends of magmatic evolution, related to spatially associated silicate intrusives (ijolitic rocks and nepheline syenite for group 1, damtjernite for group 4), rather than to a common primitive carbonatite magma (Andersen and Qvale, 1986; Andersen, 1986, 1987*a*, 1988).

It has repeatedly been suggested that a wide spectrum of derivative carbonatite magmas may evolve from a common 'primitive carbonatite magma' which may be either an alkali carbonatite magma (Le Bas, 1987) or a less alkaline, magnesium-bearing søvite magma (Twyman and Gittins, 1987). The existence of semi-independent, local carbonatite-forming trends of magmatic evolution, as seen in the Fen complex, effectively contradicts the idea of such a unique 'primitive carbonatite magma', regardless of its assumed composition. Rather, the origin of carbonatite magmas should be sought among their spatially and temporally associated igneous silicate rocks.

Conclusions

The present study has shown that contact metasomatism associated with carbonatite magmas in the Fen complex include several different processes, each inducing its characteristic mineral reactions at the magma to wall-rock interface. It is possible to relate the contact metasomatic processes observed to relative activity levels of important carbonate components in the carbonatite magma. For this purpose, carbonatite

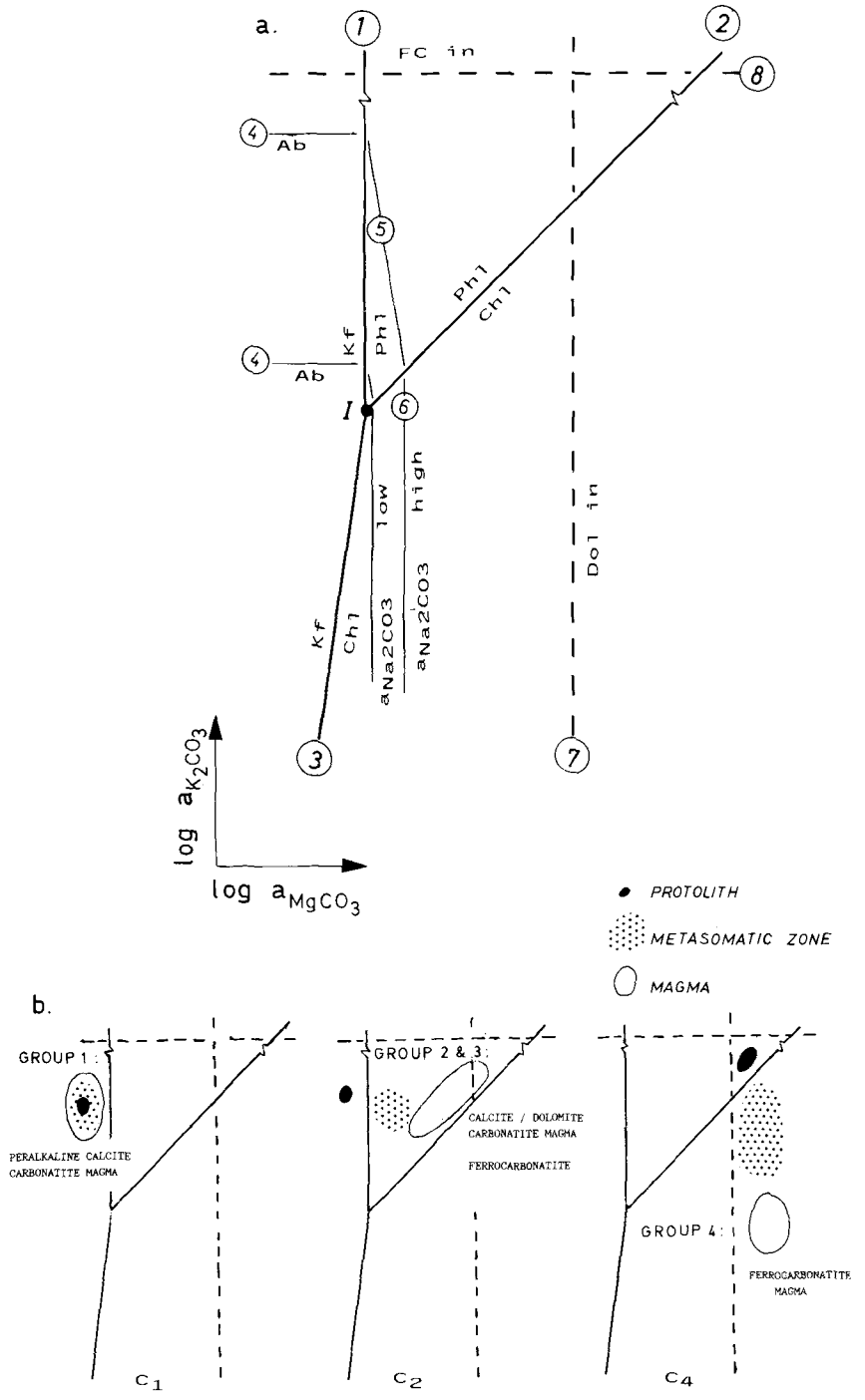
a.
FC in
Ab
Kf
Phl
Chl
I
low
high
aNa2CO3
Dol in
log aK2CO3
log aMgCO3
PROTOLITH
METASOMATIC ZONE
MAGMA
b.
GROUP 1 :
PERALKALINE CALCITE CARBONATITE MAGMA
GROUP 2 & 3 :
CALCITE / DOLOMITE CARBONATITE MAGMA
FERROCARBONATITE
GROUP 4 :
FERROCARBONATITE MAGMA
C1
C2
C4

magmas can be regarded as mixtures of the components $CaCO_3$–$MgCO_3$–$FeCO_3$–K_2CO_3–Na_2CO_3.

Among the contact metasomatic processes *alkali metasomatism* or contact fenitization s.s. is related to pyroxene søvite only. This rock-type originated from low $MgCO_3$-activity calcite carbonatite magma with high K_2CO_3 and Na_2CO_3 activities. Phlogopite- and/or amphibole-bearing søvite and dolomite carbonatite induced *magnesium metasomatism* in their wallrocks. These carbonatites crystallized from melts with higher $MgCO_3$ activity, some of which were dolomite saturated. A high $FeCO_3$ carbonatite magma, forming granular, silicate-poor ferrocarbonatite was apparently similar to the former in $a_{K_2CO_3}$ and a_{MgCO_3}, and was probably cogenetic with them.

The heterogeneous ferrocarbonatite in the eastern part of the Fen complex has caused *hydration* and *leaching of alkalis* at its contact. This magma had an elevated a_{FeCO_3}, and was dolomite-saturated and characterized by low alkali carbonate activity.

The present findings show that the metasomatic processes induced by carbonatite magmas are diverse, fenitization being one among many, and that they can convey important information on the characteristics and evolution of the carbonatite magmas. In the Fen complex, no single carbonatite magma can have been parent to all of the other carbonatite magmas which formed during evolution of the complex. This questions the validity of the concept of a unique 'primitive carbonatite magma', whatever composition is assumed for that hypothetic liquid, and suggests that the genesis of carbonatite magmas of different composition should be related to different associated silicate magmas, rather than to a single carbonatite precursor.

Acknowledgements

This work was financed by grants to the author from Norsk Hydros Fond til Vitenskapelig Forskning. Helpful discussions and critical comments from W. L. Griffin, E.-R. Neumann, P. Kresten, H. Sørensen, R. H. Verschure, C. Maijer, S. Dahlgren, A. R. Woolley, and other friends and colleagues are gratefully acknowledged.

References

Andersen, T. (1983) Iron ores in the Fen central complex, Telemark (S. Norway): Petrography, chemical evolution and conditions of equilibrium. *Norsk Geol. Tidsskr.* **63**, 73–82.

——(1984) Secondary processes in carbonatites: Petrology of 'rødberg' (hematite–calcite–dolomite carbonatite) in the Fen complex, Telemark (South Norway). *Lithos* **17**, 227–45.

——(1986) Magmatic fluids in the Fen carbonatite complex, S.E. Norway: Evidence of mid-crustal fractionation from solid and fluid inclusions in apatite. *Contrib. Mineral. Petrol.* **93**, 491–503.

——(1987*a*) Mantle and crustal components in a carbonatite complex, and the evolution of carbonatite magma: *REE* and isotopic evidence from the Fen complex, S.E. Norway. *Chem. Geol. Isotope Geosci. Sect.* **65**, 147–66.

——(1987*a*) A model for the evolution of hematite carbonatite, based on major and trace element data from the Fen complex, S.E. Norway. *Appl. Geochem.* **2**, 163–80.

——(1988) Evolution of peralkaline calcite carbonatite magma in the Fen complex, S.E. Norway. *Lithos* **22**, 99–112.

——and Qvale, H. (1986) Pyroclastic mechanisms for carbonatite intrusion: Evidence from intrusives in the Fen central complex, S.E. Norway. *J. Geol.* **94**, 762–9.

——and Sundvoll, B. (1987) Strontium and neodymium isotopic composition of an early tinguaite (nepheline microsyenite) in the Fen complex, Telemark, Southeast Norway: Age and petrogenetic implications. *Nor. geol. unders. Bull.* **409**, 29–34.

——and Taylor, P. N. (1988) Lead-isotope geochemistry of the Fen carbonatite complex, S.E. Norway: Age and petrological implications. *Geochim. Cosmochim. Acta* **52**, 209–15.

Barth, T. F. W. and Ramberg, I. B. (1966) The Fen circular complex. In *Carbonatites* (O. F. Tuttle and J. Gittins, eds.). Wiley-Interscience, New York, pp. 225–57.

FIG. 12(*a*). Mineral reactions during contact metasomatism illustrated in an uncalibrated, isothermal–isobaric log $a_{K_2CO_3}$ *vs.* log a_{MgCO_3} diagram. The numbers on the univariant curves (at P and T constant) refer to reactions in Table 8. All stability fields assume that the $CaCO_3$-activity is buffered by solid calcite. The simplifying assumptions on which this diagram is based, are discussed in the text. I represents an invariant point at constant P and T, characterized by the presence of Kf + Phl + Chl + Qz + Cc + l + v. (*b*) Activity conditions during C_1, C_2/C_3 and C_4 contact metasomatism. The diagrams constructed for each of the metasomatic processes include the activity conditions of the protolith, during contact metasomatism and in the magmas responsible. The fields for the protoliths have been deduced from the pre-metasomatic mineral assemblages. The conditions *during* contact metasomatism were derived from the mineralogies of the contact metasomatic zones. The approximate fields for the magmas are based on the assumption that the activity shifts during contact metasomatism (from protolith to metasomatic zone) are directed towards the fields of the magmas responsible, as discussed in the text.

Bergstøl, S. and Svinndal, S. (1960) The carbonatite and peralkaline rocks of the Fen area. *Nor. geol. unders.* **208**, 99–105.

Brøgger, W. C. (1921) *Die Eruptivgesteine des Kristianiagebietes, IV. Das Fengebiet in Telemark, Norwegen.* Vit. Selsk. Skr., I Mat. Nat. Klasse 1920, 1, Kristiania, 494 pp.

Castellan, G. W. (1971) *Physical Chemistry*, 2nd ed. Addison-Wesley. 866 pp.

Dahlgren, S. (1978) Nordagutu, bedrock map 1:50 000 (preliminary edition). *Nor. geol. Unders.*

——(1987) *The Satellitic Intrusions in the Fen carbonatite Alkaline Rock Province, Telemark, Southeastern Norway.* Unpubl. Cand. Scient. Thesis, University of Oslo.

Dawson, J. B. (1962) Sodium carbonatite lavas from Oldoinyo Lengai, Tanganyika. *Nature* **195**, 1075–6.

——(1964) Reactivity of the cations in carbonate magmas. *Geol. Assoc. Canada Proc.* **15**, 103–13.

——Garson, M. S. and Roberts, B. (1987) Altered former alkalic carbonatite lava from Oldoynio Lengai, Tanzania: Inferences for calcite carbonatite lavas. *Geology* **15**, 765–8.

v. Eckermann, H. (1948) The alkaline district of Alnö Island. *Sver. Geol. Unders. Ser. Ca.* **36**, 176 pp.

Gittins, J. (1979) Problems inherent in the application of calcite-dolomite geothermometry to carbonatites. *Contrib. Mineral. Petrol.* **69**, 1–4.

——and McKie, D. (1980) Alkalic carbonatite magmas: Oldoinyo Lengai and its wider applicability. *Lithos* **13**, 213–5.

Greenwood, H. J. (1976) Metamorphism at moderate temperatures and pressures. In *The evolution of the crystalline rocks* (D. K. Bailey and R. MacDonald, eds.). Academic Press, London, pp. 187–259.

Heinrich, E. W. (1966) *The geology of carbonatites.* Rand McNally and Co., Chicago, 555 pp.

Hay, R. L. (1978) Melilitite–carbonatite tuffs in the Laetolil beds of Tanzania. *Contrib. Mineral. Petrol.* **67**, 357–67.

Hey, M. H. (1954) A new review of the chlorites. *Mineral. Mag.* **30**, 277–92.

Kjarsgaard, B. A. and Hamilton, D. L. (1988) Liquid immiscibility and the origin of alkali poor carbonatites. Ibid. **52**, 43–55.

Kresten, P. (1979) *The Alnö complex. Discussion of the main features, bibliography, excursion guide.* Nordic Carbonatite Symposium, Alnö 1979, 67 pp.

——(1988) The chemistry of fenitization: Examples from Fen, Norway. *Chem. Geol.* **68**, 329–49.

——and Morogan, V. (1986) Fenitization at the Fen complex, southern Norway. *Lithos* **19**, 27–42.

Le Bas, M. J. (1977) *Carbonatite–Nephelinite Volcanism.* Wiley, New York.

——(1981) Carbonatite magmas. *Mineral. Mag.* **44**, 133–40.

——(1987) Nephelinites and carbonatites. In *Alkaline igneous rocks* (J. G. Fitton and B. G. J. Upton, eds.). Geol. Soc. Spec. Publ. No. 30, Blackwell, Oxford, pp. 53–84.

McKie, D. (1966) Fenitization. In *Carbonatites* (O. F. Tuttle and J. Gittins, eds.). Wiley-Interscience, New York, pp. 261–94.

Mitchell, R. H. and Brunfelt, A. O. (1975) Rare earth element geochemistry of the Fen alkaline complex, Norway. *Contrib. Mineral. Petrol.* **52**, 247–59.

Morogan, V. (1988) Fenitization, hallmark of the ijolite–carbonatite magmatic association. *Medd. Stockh. Universitets Geol. Inst.* **274**.

Ramberg, I. B. (1973) Gravity studies of the Fen complex, Norway, and their petrological significance. *Contrib. Mineral. Petrol.* **38**, 115–34.

Rice, J. M. (1977) Progressive metamorphism of impure dolomitic limestone in the Maryville aureol, Montana. *Am. J. Sci.* **277**, 1–24.

Sæther, E. (1957) *The alkaline rock province of the Fen area in southern Norway.* Det Kgl. Nor. Vit. Selsk. Skr. 1957, 1, 148 pp.

Secher, K. and Larsen, L. M. (1980) Geology and mineralogy of the Sarfartôq carbonatite complex, East Greenland. *Lithos* **13**, 199–212.

Statham, P. J. (1976) A comparative study of techniques for quantitative analysis of X-ray spectra obtained with a Si(Li) detector. *X-ray Spectrom.* **5**, 16–28.

Treiman, A. H. and Essene, E. J. (1985) The Oka carbonatite complex, Quebec: geology and evidence for silicate-carbonate liquid immiscibility. *Am. Mineral.* **70**, 1101–13.

——and Schedl, A. (1983) Properties of carbonatite magma and processes in carbonatite magma chambers. *J. Geol.* **91**, 437–17.

Twyman, J. D. and Gittins, J. (1987) Alkalic carbonatite magmas: parental or derivative? In *Alkaline igneous rocks* (J. G. Fitton and B. G. J. Upton, eds.). Geol. Soc. Spec. Publ. No. 30, Blackwell, Oxford, pp. 85–94.

Verschure, R. H. and Maijer, C. (1984) Pluri-metasomatic resetting of Rb–Sr whole-rock systems around the Fen peralkaline–carbonatitic ring-complex, Telemark, South Norway. *Terra Cognita* **4**, 191–2.

Verwoerd, W. J. (1966) Fenitization of basic igneous rocks. In *Carbonatites* (O. F. Tuttle and J. Gittins, eds.). Interscience, New York, pp. 295–308.

Woolley, A. R. (1982) A discussion of carbonatite evolution and nomenclature, and the generation of sodic and potassic fenites. *Mineral. Mag.* **46**, 13–17.

Wyllie, P. J. (1966) Experimental studies of carbonatite problems: The origin and differentiation of carbonatite magmas. In *Carbonatites* (O. F. Tuttle and J. Gittins, eds.). Interscience, New York, pp. 311–52.

[*Manuscript received 26 October 1988: revised 4 January 1989*]